Contents lists available at ScienceDirect

Applied Catalysis B: Environmental

Research Paper

Identification of homogeneous $[Co_4(H_2O)_4(HPMIDA)_2(PMIDA)_2]^{6-}$ as an effective molecular-light-driven water oxidation catalyst

Qian Xu[a], Hui Li[a], Le Chi[a], Liugen Zhang[a], Zheng Wan[a], Yong Ding[b], Jide Wang[a,*]

[a] Key Laboratory of Oil and Gas Fine Chemicals, Ministry of Education & Xinjiang Uygur Autonomous Region, College of Chemistry and Chemical Engineering of Xinjiang University, Urumqi, 830046, China
[b] College of Chemistry and Chemical Engineering of Lanzhou University, Lanzhou, 730000,China

ABSTRACT

Transition-metal complexes, especially cobalt complexes, are used as precatalysts in homogeneous water oxidation catalysis. However, a practical method of identifying the effective active species in cobalt-complex homogeneous catalysts under highly oxidizing conditions have not yet been established. In this work, $(H_3O)_6 \cdot [Co_4(H_2O)_4(HPMIDA)_2(PMIDA)_2] \cdot 2H_2O$ (**1**) was introduced, and its photocatalytic performance was evaluated. The compound exhibited effective water oxidation catalysis, with a turnover number of 661.5 at pH 9.0 using $[Ru(bpy)_3](ClO_4)_2$ as photosensitizers and sodium persulfate as sacrificial electron acceptor. Accordingly, **1** was used as target catalysts, and the active species was thoroughly investigated under catalytic conditions. The stability of **1** was further tested and confirmed by a series of experiments (cyclic voltammetry (CV), ultraviolet–visible (UV–vis) spectrometry, dynamic light-scattering (DLS), aging experiments, and extraction techniques). Results showed that **1** maintained its structural integrity under the given photocatalytic conditions. Furthermore, cathodic adsorptive stripping voltammetry and inductively coupled plasma-mass spectrometry were used to quantify the amount of Co^{2+} ions released from **1** into borate buffer after oxidation. The pH dependence of the oxygen-evolution performance of **1** and other cobalt species were then compared. Data collectively revealed that **1** was stable during water oxidation; it did not release free Co^{2+} ions and was not hydrolyzed to cobalt oxide or hydroxide, thereby confirming that **1** was the effective active species in water-oxidation catalysis.

© 2016 Elsevier B.V. All rights reserved.

1. Introduction

Hydrogen is the cleanest form of energy. Water splitting obtains mass production of hydrogen efficiently [1,2]. The process is composed of two half reactions: (i) the four-electron oxidation of water:

$$2H_2O \rightarrow O_2 + 4H^+ + 4e^- \tag{1}$$

and (ii) the reduction of four protons:

$$4H^+ + 4e^- \rightarrow 2H_2 \tag{2}$$

Water oxidation delays the overall water splitting for the two half reactions, because it is a more complex chemical reaction than proton reduction and provides four electrons per molecule [3–7]. Therefore, a considerable number of studies have investigated efficient artificial water oxidation catalysts (WOCs) to obtain low-cost renewable energy sources [8–12]. In the past few decades, homo-geneous and heterogeneous catalysts for water oxidation have made great improvement, based on non-noble metals (Fe, Co, Ni, etc.) [13–20]. Specifically, the homogeneous Co complexes, such as cobalt polyoxometalates [21–24], organic cobalt phosphonates [25,26], and organic/inorganic cobalt complexes [27,28], have been reported as efficient and stable catalysts for water oxidation. However, most WOCs, especially organic/inorganic cobalt complexes, have been tested if they perform as molecular catalysts [29–31]. A recent study implied that the effective catalytic species in water oxidation catalysis are Co^{2+} or CoO_x [32,33]. In situ formed CoO_x or $Co(OH)_x$ as WOCs have been reported by Ding et al. [34] These catalysts were generated from the decomposition of Salen Co (II) under oxidizing conditions. In addition, Fukuzumi et al. [35] synthesized and characterized four water-soluble cobalt complexes: $[Co^{II}(Me_6tren)(OH_2)]^{2+}$ (**a**), $[Co^{III}(Cp^*)(bpy)(OH_2)]^{2+}$ (**b**), $[Co^{II}(12-TMC)]^{2+}$ (**c**), and $[Co^{II}(13-TMC)]^{2+}$ (**d**). These experimental results indicated that the mononuclear cobalt complexes with organic ligands **a** and **b** act as efficient precatalysts. Both were oxidized to produce actual reactive catalysts during the photocatalytic water oxidation, *i.e.*, nanoparticles composed of $Co(OH)_x$. Initially,

* Corresponding author.
  E-mail address: awangjd@sina.cn (J. Wang).

few mechanisms concerning the evolution of CoO_x and $Co(OH)_x$ are available. The process is regarded as a cobalt–oxo/hydroxo-based solid incorporated with excess counter-cations and −anions. Meanwhile, these active species are conductive to release oxygen. Therefore, the identification of effective catalytic species for homogeneous water oxidation is of great importance. In this regard, Hill et al. [36] developed a series of new techniques (cathodic adsorptive stripping voltammetry (CAdSV) and inductively coupled plasma mass spectrometry (ICP-MS)) to distinguish different types of WOCs in homogeneous reaction. They provided strong evidence that polyoxometalate anions functioned as a molecular catalysts and not a CoO_x precursor.

Although most of organic/inorganic cobalt-based complexes are proven to be precatalysts in water oxidation process, the high activity observed in this system encourages further work for deeper mechanistic understanding. Thus, the development of more practical devices for higher efficiency of fuel generation from renewable sources is urgent.

The current work almost focused on the investigation of the stability of catalysts and evaluation of their performance. However, few reports questioned the effectiveness of active species to contribute in catalytic process. Measuring the effectiveness of active species is difficult. It needs not only differentiating a homogeneous catalyst from a heterogeneous one under oxidizing conditions, but also distinguishing particular molecular species generated in solution during turnover, especially when the techniques to study the effective active species are not enough. Therefore, devising some practical means to examine the active species from reactants and decomposition products and reveal which active species is effective in the catalysis reaction are of great significance. Moreover, the catalytic activity of cobalt complexes can be conducted on the atomic level and kept in the molecular water oxidation catalysts by selecting an organic ligand, such that these compounds are robust under highly oxidizing conditions. Hence, we chose $[Co_4(H_2O)_4(HPMIDA)_2(PMIDA)_2]^{6-}$ (**1**) as target catalysts and studied its water oxidation performance. In this article, a series of techniques were applied to study the effective active species and demonstrated that **1** could efficiently catalyze water oxidation. These technologies include CAdSV and ICP-MS, which were applied to quantify the amount of Co^{2+} leaching from **1**. The pH-dependence of **1** and other cobalt species was also compared. The experimental results indicated that Co^{2+} or CoO_x would not act as active species.
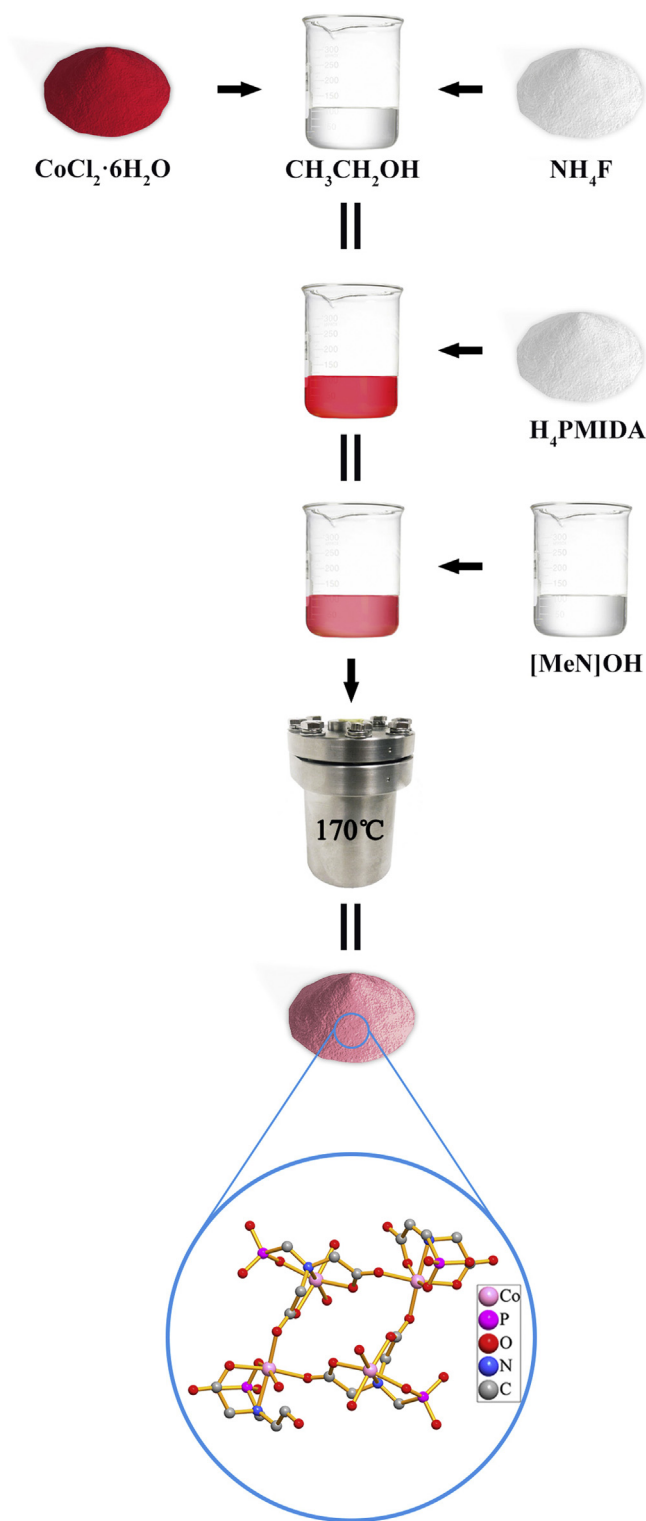
2. Experimental

2.1. Synthesis

Specific procedure for synthesis was done according to [37]. A 0.238 g $CoCl_2 \cdot 6H_2O$ and 0.148 g NH_4F were dissolved in 10 mL ethanol, followed by the addition of 0.234 g *N*-(phosphonomethyl) iminodiacetic acid (H$_4$PMIDA) with vigorous stirring. Subsequently, 0.6 mL of [Me$_4$N]OH solution (15% in water) was added to the resulting solution, followed by stirring until a homogeneous reaction mixture was formed to the molar radio of $CoCl_2 \cdot 6H_2O$:NH$_4$F:H$_4$PMIDA:[Me$_4$N]OH is 1:4:1:1. The reaction mixture was crystallized in a 20 mL PTFE-lined acid digestion bomb at 170 °C for 5 d. The crystalline product **1** was collected by vacuum filtration, thoroughly washed with ethanol, and air dried (Scheme 1).

2.2. Photocatalytic water oxidation

Photocatalytic water oxidation was performed as follows: compound **1** was added to a buffer solution (80 mM borate buffer, pH 8.0–10.0), which contains Na$_2$S$_2$O$_8$ (5 mM) and [Ru(bpy)$_3$](ClO$_4$)$_2$

Scheme 1. Schematic of the synthetic procedures.

(1 mM) purged with Ar gas for 10 min in a flask (~20 mL) sealed with a rubber septum. The reaction was started by irradiating the solution with a Xe lamp (300 W, 26.4 mW/cm^2) by a transmitting glass filter ($\lambda \geq 420$ nm) at room temperature. After each sampling time, 100 μL of Ar was injected into the flask, and the same volume of the gas sample in the headspace of the flask was withdrawn by a gas tight syringe and used for gas chromatography analysis. O$_2$ in the sampled gas was separated by passing it through a
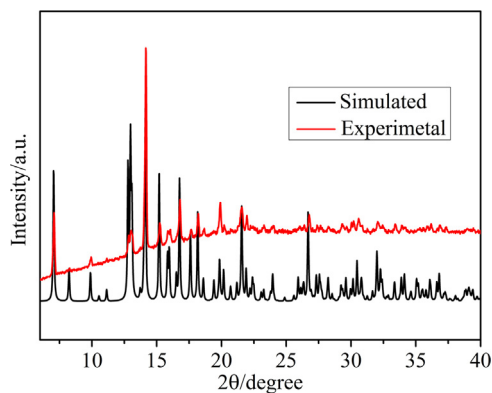
Fig 1. XRD patterns of **1**.

molecular sieve with 5 Å columns and an Ar carrier gas. The levels were quantified by a thermal conductivity detector (Shimadzu GC-14B). The total amount of evolved O_2 was calculated from the O_2 concentration in the headspace gas.

2.3. Electrochemical synthesis of CoO_x

CoO_x was synthesized according to [38], and CoO_x was deposited on fluorine-doped tin oxide (FTO). Electrolysis proceeded at 1.29 V (vs. Ag/AgCl) without stirring in 0.1 M sodium phosphate buffer (pH 7) solution containing 0.5 mM $Co(NO_3)_2 \cdot 6H_2O$. During 7–8 h, a dark coating form on the FTO surface, which was dried in air then removed from the FTO electrode with a razor blade.

2.4. Characterization techniques

CV measurements were performed in a typical three-electrode cell, with platinum wire as counter electrode and Ag/AgCl as reference electrode. The electrochemical experiments were performed on a CHI600D workstation (CH Instruments). The sweep rate for CVs was 100 mV/s, unless otherwise stated. DLS measurements were performed with a Zetasizer Nano S90 instrument (Malvern Instruments Ltd.) for the reaction solution. The UV–vis absorption spectra were recorded on UV-2550 spectrophotometer (Shimadzu). Elemental analyses of Co were performed on an ICP-4300DV ICP atomic emission spectrometer.

3. Results and discussion

3.1. Characterization

The X-ray diffraction (XRD) pattern is shown in Fig. 1. All diffraction peaks were consistent with the simulation, indicating the high purity of the synthesized sample **1**.

Scanning electron microscopy (SEM) and energy-dispersive X-ray analysis (EDX) spectra were applied to study the morphology and composition of the electrode coating formed by electrochemical deposition in the presence of Co^{2+} ions (Fig. S1).The SEM image of CoO_x (Fig. S1a) revealed that it consists of individual microspheres with smooth surface. EDX indicated that only Co, O, P, and K exist in the material, with Co/O/P ratio of 2.85:1:4.61 (Fig. S1b). These data were consistent with those reported by Nocera et al. [38].

3.2. Electrochemical properties of 1

CV was applied to further analyze the electrochemical properties of **1**. The CV curve in Fig. 2a shows one reversible wave at ∼0.7 V (vs. Ag/AgCl), which is assigned to $Co^{II/III}/Co^{III/II}$ oxidation. The maximum current of ∼0.25 mA was attained at 1.20 V. The onset of the
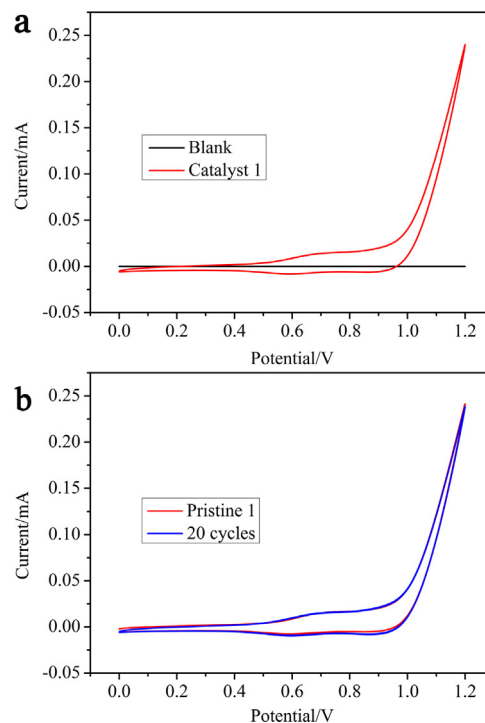

Fig. 2. (a) CV of 80 mM sodium borate buffer solution at pH 9.0 with 0.1 mM of **1**. (b) CV after 20 cycles with 0.1 mM in 80 mM sodium borate buffer solution (pH 9.0) (The scan rate was 100 mV/s.). Ag/AgCl was used as the reference electrode.

catalytic wave attributed to water oxidation is observed at ∼0.4 V (vs. Ag/AgCl). By contrast, the blank control experiment showed a minimum current in the same buffered solution. Results clearly indicated that **1** can catalyze water oxidation. After 20 cycles, catalytic current remained unchanged (Fig. 2b), indicating that electro deposition of active species did not exist and that **1** maintained its electrochemical stability.

3.3. Photocatalytic water oxidation

The photocatalytic activity of **1** was studied in a borate buffer (80 mM) with a $[Ru(bpy)_3]^{2+}$-$S_2O_8^{2-}$ system. Fig. 3a shows that the highest amount of O_2 is obtained at pH 9.0, and that the rate constant is 0.22×10^{-3} mol/(L min). Generally, the reaction of $4[Ru(bpy)_3]^{3+} + 2H_2O \rightarrow 4[Ru(bpy)_3]^{2+} + O_2 + 4H^+$ was important for oxygen evolution; the high pH value positively contributed to water oxidation in thermodynamics [39,40]. However, the catalytic activity was decreased by increasing the pH value from 9.0 to 10.0; the rate constant was decreased to 0.20×10^{-3} mol/(L min). According to the first-order decay kinetics, a higher pH value will lead to the acceleration of $[Ru(bpy)_3]^{3+}$ decomposition; the rate constant rely on pH and the buffer nature to a smaller extent [41]. As shown in Fig. 3b, the amount of oxygen evolution increased by approximately 5 min, and then started to stabilize after 6 min. After the decomposition of photosensitizers (see Section 3.4) and consumption of persulfate, the amount of evolved O_2 could reach a certain value. A maximum oxygen yield of 53%, an oxygen evolution amount of 13.2 μmol, and a turnover number (TON) of 661.5 were obtained when the concentration of **1** was increased to 2.0 μM, which achieved a good performance (Table S1) for light-driven water oxidation among the documented cobalt complexes to date. The high TON value reveals that **1** is an effective water oxidation catalyst. The photocatalytic water oxidation was also investigated in the absence of **1**. Oxygen evolution was not detected after 6 min of
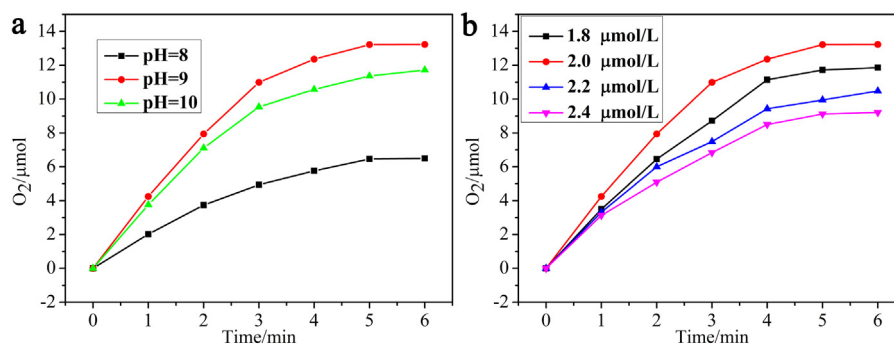
Fig. 3. (a) Kinetics of O_2 evolution of the photocatalytic system with different pH conditions with 2.0 μM of **1** (pH 8.0, black; pH 9.0, red; pH 10.0, green). Conditions: Xe lamp ($\lambda \geq 420$ nm), 1.0 mM [Ru(bpy)$_3$](ClO$_4$)$_2$, 5.0 mM Na$_2$S$_2$O$_8$, and 80 mM sodium borate buffer (pH 9.0). The total reaction volume is 10 mL and the overall volume is 20 mL. (b) The kinetics of O_2 evolution of the photocatalytic system with different concentrations of **1** (1.8 μM, black; 2.0 μM, red; 2.2 μM, blue; 2.4 μM, pink). Conditions: Xe lamp ($\lambda \geq 420$ nm), 1.0 mM [Ru(bpy)$_3$](ClO$_4$)$_2$, 5.0 mM Na$_2$S$_2$O$_8$, 80 mM sodium borate buffer (pH 9.0). The total reaction volume is 10 mL and the overall volume is 20 mL (For interpretation of the references to colour in this figure legend, the reader is referred to the web version of this article.)
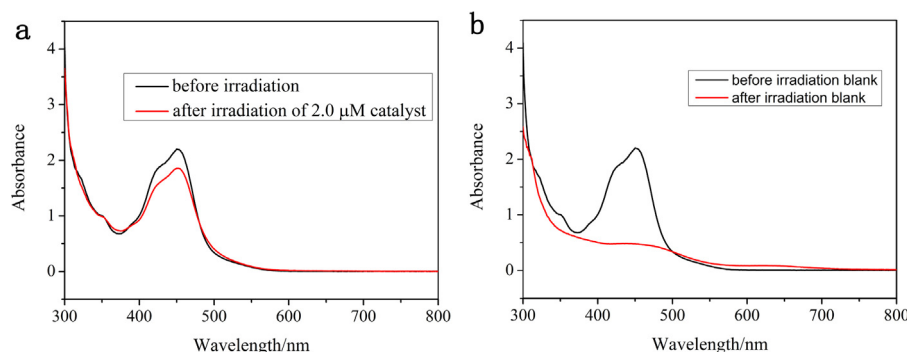

Fig. 4. (a) UV–vis spectra during the photocatalytic O_2 evolution with **1**. Absorption of the aqueous borate buffer solution (pH 8.5, 80 mM) containing [Ru(bpy)$_3$](ClO$_4$)$_2$ (1 mM), Na$_2$S$_2$O$_8$ (5 mM), and **1** (2.0 μM) (black); absorption of the above mentioned solution after 6 min of irradiation (red). (b) UV–vis spectra during the photocatalytic O_2 evolution without any catalysts. Absorption of aqueous borate buffer solution (pH 9.0, 80 mM) containing [Ru(bpy)$_3$](ClO$_4$)$_2$ (1 mM) and Na$_2$S$_2$O$_8$ (5 mM) (black); absorption of above mentioned solution after 6 min of irradiation (red). (For interpretation of the references to colour in this figure legend, the reader is referred to the web version of this article.)
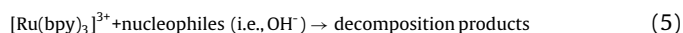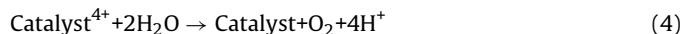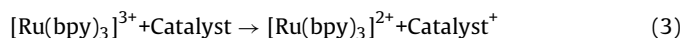
irradiation without **1**. In addition, oxygen was not observed without a photosensitizer or sodium peroxodisulfate.

The overall process for water oxidation is shown in Scheme 2. The excited photosensitizers [Ru(bpy)$_3$]$^{2+*}$ were generated from [Ru(bpy)$_3$]$^{2+}$ under illumination. The two [Ru(bpy)$_3$]$^{2+*}$ reacted with sodium peroxodisulfate and generated two [Ru(bpy)$_3$]$^{3+}$, two SO$_4$$^{2-}$, and two radical ion SO$_4$$^-$. The latter, which was also a strong oxidant, oxidized another two [Ru(bpy)$_3$]$^{2+}$ to give two more [Ru(bpy)$_3$]$^{3+}$ accompanying radical anions SO$_4$$^-$· that converted into SO$_4$$^{2-}$. The [Ru(bpy)$_3$]$^{3+}$ sequentially obtained four electrons from the catalyst and oxidized water to release dioxygen and restore [Ru(bpy)$_3$]$^{2+}$ before proceeding to another cycle of water oxidation.

3.4. Photosensitizer decomposition

According to [42], the photosensitizer [Ru(bpy)$_3$]$^{3+}$ will be consumed by two routes. First, the photosensitizer reacts with the catalyst, thereby transferring its electron vacancy to the catalyst species (for simplicity, herein referred to as Catalyst) and regenerates [Ru(bpy)$_3$]$^{2+}$ (Eq. (3)). Alternatively, self-quenching and decomposition occur via the nucleophilic attack of OH$^-$ under neutral or basic condition (Eq. (5)). The simplest case assumes that the active state of the catalyst toward water oxidation is four-time oxidized Catalyst^{4+} species; the hole-scavenging reaction in Eq. (3) must be repeated four times to accumulate the catalyst structure, and finally Eq. (4) can occur. If the rate constant of Eq. (5) is much faster than the process in Eq. (3), the process of decomposition
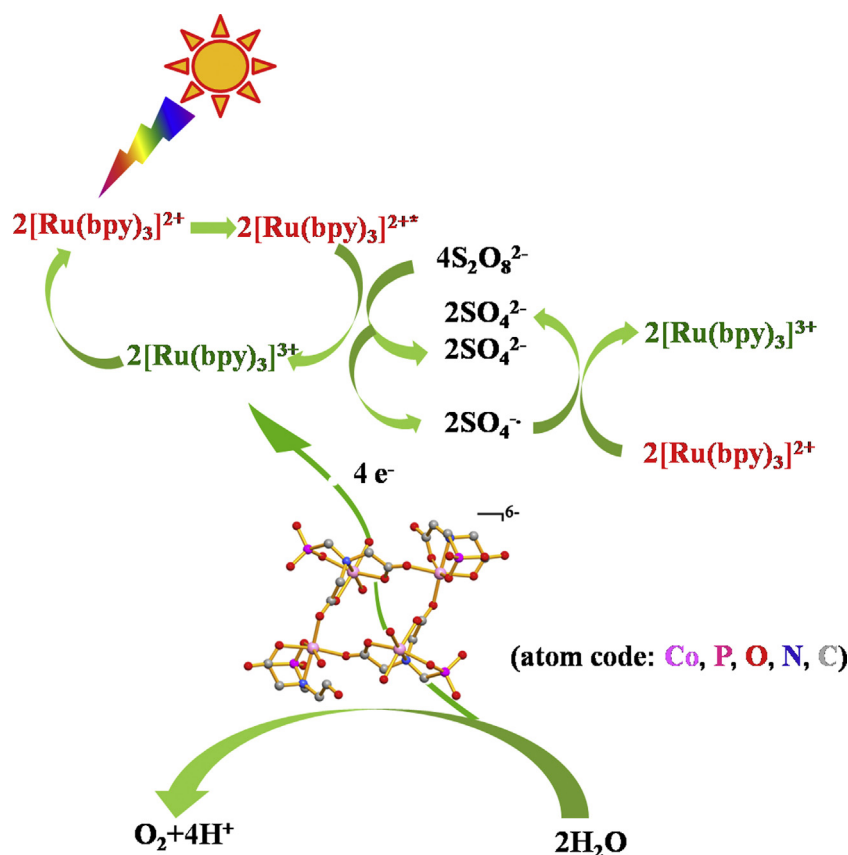
of the photosensitizer can lead to full deactivation of the photocatalytic ability of the system, which finally affects the O_2 yield. Therefore, WOCs should be identified to protect the photosensitizer from irreversible decomposition and improve O_2 evolution yield [43,44]. UV–vis spectra showed the effect of adding **1** to the reaction solution. After 6 min of illumination, [Ru(bpy)$_3$]$^{2+}$ concentration decreased by 15% (Fig. 4a). By contrast, the control experiment showed the decomposition of [Ru(bpy)$_3$]$^{2+}$ by up to 78% in the absence of a catalyst (Fig. 4b). The UV–vis evidence support that **1** could be protected against photosensitizer decomposition.

$$[Ru(bpy)_3]^{3+} + Catalyst \rightarrow [Ru(bpy)_3]^{2+} + Catalyst^+ \qquad (3)$$

$$Catalyst^{4+} + 2H_2O \rightarrow Catalyst + O_2 + 4H^+ \qquad (4)$$

$$[Ru(bpy)_3]^{3+} + nucleophiles \ (i.e., OH^-) \rightarrow decomposition \ products \qquad (5)$$

3.5. Stability studies of 1

Multiple experiments were employed to examine the effective active species of WOCs in water oxidation. We hypothesized that **1** is the molecular catalyst that functions as the catalytic active species, such that cobalt ions or cobalt oxides were not released from **1**. We investigated the catalytic behavior of **1** and compared the oxygen evolution performance of three possible catalysts.

First, we tested the stability of **1** by UV–vis spectrometry with different irradiation times (0–60 min). As shown in Fig. 5, the UV–vis spectra remained unchanged with time even after 60 min, thereby supporting the stability of the **1** in borate buffer at pH 9.0. Fig. 5 shows the characteristic absorbance of **1** observed at

Scheme 2. Light-driven water oxidation by **1** with [Ru(bpy)$_3$]$^{2+}$ as photosensitizers and sodium peroxodisulfate as the sacrificial electron acceptor.
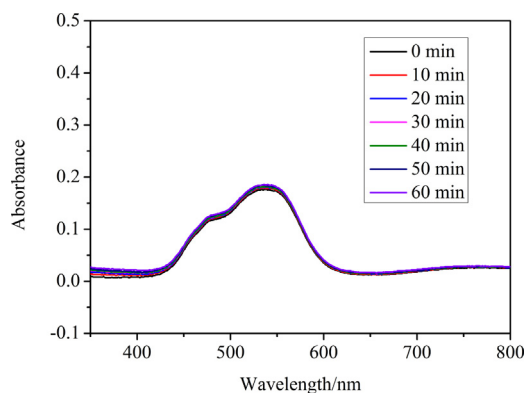

Fig. 5. UV–vis spectra of 0.5 mM of **1** in 80 mM borate buffer (pH 9.0) and 5 mM Na$_2$S$_2$O$_8$ with different irradiation times (0, 10, 20, 30, 40, 50 and 60 min).

550 nm by UV–vis spectra. In photocatalytic O$_2$ evolution process, the UV–vis spectra of **1** with different reaction times were devised as well (Fig. S3), which had not changed significantly at 550 nm. Second, freshly prepared 1 mM [Ru(bpy)$_3$](ClO$_4$)$_2$ and 5 mM Na$_2$S$_2$O$_8$ were added to the aged solution to examine the catalytic activity; 12.3 μmol O$_2$, 49% O$_2$ yield, and TON of 614 were obtained (Fig. S2). Similar kinetics of oxygen for both freshly prepared and 3 h-aged solutions in 80 mM borate buffer at pH 9.0 further proved that the catalyst was stable.

Third, DLS measurement was performed in a solution of 2.0 μM **1** or Co(NO$_3$)$_2$, 1 mM [Ru(bpy)$_3$](ClO$_4$)$_2$, and 5 mM Na$_2$S$_2$O$_8$ in a 80 mM borate buffer (pH 9.0) after 6 min of irradiation with a Xe lamp. DLS studies indicated that in the reaction solution containing **1**, nanoparticles could not be detected after photocatalytic water oxidation (Fig. 6a). By contrast, the size of formed particles was

160 nm when Co(NO$_3$)$_2$ was used as a catalyst (Fig. 6b). These evidence provide that cobalt hydroxide or oxide nanoparticles are not generated by the hydrolytic decomposition of **1** after photocatalytic experiments.

Hill et al. [36] devised an extraction method to address catalysis by soluble molecular species versus insoluble metal oxides or soluble hydrated metal cations as catalysts for reactions in aqueous solutions. A similar experiment was applied to extract **1** from the aqueous solution. This method is a two-step process where a soluble, anionic catalyst was separated from the solution containing all species present during turnover. Next, the remaining cobalt solution containing species was quantified. A 2 μM of **1** was aged in 80 mM sodium borate buffer (pH 9.0) for 3 h, followed by using tetra-*n*-heptylammonium nitrate (THpANO$_3$, in toluene) to extract **1** from the aqueous layer. After extraction from the aqueous solution of **1**, ICP-MS was applied to quantify the amount of Co-containing species remaining in the solution. The THpANO$_3$/toluene extraction and ICP-MS analysis result indicated yielded concentration of cobalt at 0.07 μM remaining in the reaction solution. Moreover, CAdSV was applied to further verify the amount of cobalt ion, which was initially reported by Finke [33]. The yield concentration of cobalt ion residue was 0.07 μM as well. The CAdSV and ICP-MS analysis results indicated that less than <0.35% of the catalyst could have decomposed to release Co^{2+} ions in the borate buffer. Experiment result shows that rolling out the dissociated Co^{2+} ions may have caused water oxidation activity. This experiment did not detect O$_2$ evolution.

The kinetic behavior was evaluated in terms of different catalysis between each catalytic species under specific conditions to present further evidence, differentiating from Co^{2+} (aq), CoO$_x$, or other possible decomposition products (Table 1). The pH-dependence of **1** was compared with that of other species.
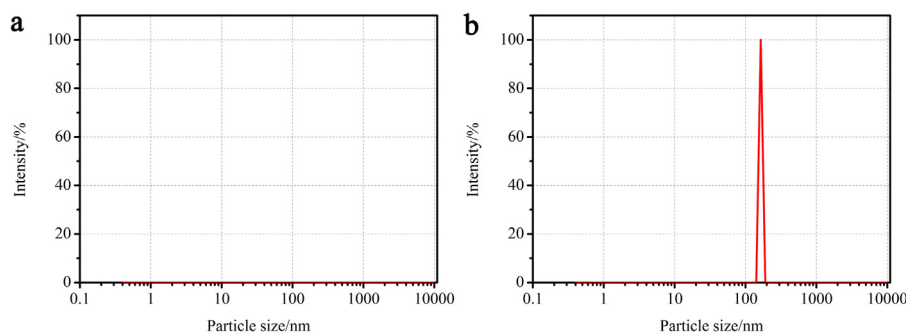
Fig. 6. Particle size distribution (intensity, %) obtained from DLS measurement for post-reaction solutions containing (a) 2 μM **1** or (b) Co(NO$_3$)$_2$ as catalysts with 1 mM [Ru(bpy)$_3$](ClO$_4$)$_2$ in a 80 mM borate buffer (pH 9.0) and 5 mM Na$_2$S$_2$O$_8$.

Table 1
Light-driven water oxidation activity of **1**, Co^{2+} (aq), and CoO$_x$ at different pH[a].

Entry	Complex	Complex concentration/μM	pH	Buffer/mM	TON	O$_2$ yield/%
1	1	2.0	9.0	80 NaBi	661.5	53
2	1/aged 3 h[b]	2.0	9.0	80 NaBi	614.0	49
3	1	2.0	8.0	80 NaBi	325.0	26
4	1	2.0	7.0	80 NaBi	18.5	2
5	Co(NO$_3$)$_2$	8.0	9.0	80 NaBi	244.3	78
6	Co(NO$_3$)$_2$	8.0	8.0	80 NaBi	139.1	44
7	Co(NO$_3$)$_2$	8.0	7.6	80 NaBi	7.1	22
8	Co(NO$_3$)$_2$	2.0	8.0	80 NaBi	149.5	12
	Co(NO$_3$)$_2$	2.0	7.0	80 NaBi	21.5	2
10	CoO$_x$[c]	8[d]	9.0	80 NaBi	43.9	14
11	CoO$_x$[c]	8[d]	8.0	80 NaBi	34.1	11
12	CoO$_x$[c]	8[d]	7.0	80 NaBi	23.4	8

[a] Conditions: 1 mM [Ru(bpy)$_3$](ClO$_4$)$_2$, 5 mM Na$_2$S$_2$O$_8$, Xe lamp (λ ≥ 420 nm), 10 mL total solution volume, all stock solutions prepared in DI water.
[b] Aged in the corresponding buffer solution.
[c] CoO$_x$ was prepared by electrochemical deposition as described in the Experimental Section.
[d] Not soluble, the suspension was obtained after 30 min of sonication, 8 μM of Co^{2+} were used for catalytic reaction. The errors are calculated as the standard deviation from multiple experiments.

Generally, the pH-dependence of O$_2$ yield or O$_2$ evolution number (TON) was consistent with the presence of different catalytically active species during turnover. Thus, the pH-dependence of O$_2$ or TON for **1**, Co^{2+} (aq), and CoO$_x$ as catalysts were compared. Table 1 shows that the activity of **1** strongly depends on pH. Entries 3 and 4 demonstrated that when pH is increased from 7.0 to 8.0 and other conditions are held constant, the O$_2$ yield and TON increase by 20-fold. By contrast, O$_2$ yield and TON of Co(NO$_3$)$_2$ or CoO$_x$ were weakly dependent on pH because O$_2$ yield and TON increased by only ~1.5- and ~2-fold, respectively, at the same conditions. The different degrees of pH dependence of kinetic behavior indicated that the catalytic activity from **1** is not a result of either Co^{2+} (aq) or CoO$_x$.

4. Conclusions

The molecular catalyst [Co$_4$(H$_2$O)$_4$(HPMIDA)$_2$(PMIDA)$_2$]$^{6-}$ was selected, and its photocatalytic performance was evaluated. The catalyst exhibited high photocatalytic oxygen evolution with a high TON of 661.5. CV results revealed that **1** contributed to the catalysis of water oxidation and remained electrochemically stable. A series of experiments, including UV–vis spectrometry, aging experiment, DLS, and extraction techniques were applied to test the oxygen evolution performance and stability. These collective studies support that **1** maintains its structural integrity during the entire water oxidation reaction.

The complementary techniques, CAdSV and THpANO$_3$/toluene extraction, followed by ICP-MS determination, were used to quantify the released number of cobalt species in the borate buffer after oxidation. Both sets of results showed that the remaining cobalt concentration in the solution was 0.07 μM, which could not be involved in water oxidation.

Furthermore, the oxygen evolution performance and pH dependence of **1** were compared with other cobalt species. These evidence showed that the catalytic activity of **1** was completely different from those of other species. In addition, water oxidation was not generated by either Co^{2+} (aq) or CoO$_x$.

All evidence revealed that **1** exhibits high evolution performance of photocatalytic oxygen and functions as an effective molecular water oxidation catalyst, which is stable during water oxidation; the catalyst neither releases free Co^{2+} ions nor hydrolyzes into cobalt oxide or hydroxide.

Acknowledgement

Appendix A. Supplementary data

Supplementary data associated with this article can be found, in the online version, at http://dx.doi.org/10.1016/j.apcatb.2016.09.056.

References

[1] A.J. Bard, M.A. Fox, Artificial photosynthesis: solar splitting of water to hydrogen and oxygen, Acc. Chem. Res. 28 (1995) 141–145.
[2] M. Yagi, M. Kaneko, Molecular catalysts for water oxidation, Chem. Rev. 101 (2001) 21–36.

[3] P. Du, R. Eisenberg, Catalysts made of earth-abundant elements (Co, Ni, Fe) for water splitting: recent progress and future challenges, Energy Environ. Sci. 5 (2012) 6012–6021.

[4] Y. Ma, X. Wang, Y. Jia, X. Chen, H. Han, C. Li, Titanium dioxide-based nanomaterials for photocatalytic fuel generations, Chem. Rev. 114 (2014) 9987–10043.

[5] J. Huang, Y. Ding, X. Luo, Y. Feng, Solvation effect promoted formation of p-n junction between WO_3 and FeOOH: a high performance photoanode for water oxidation, J. Catal. 333 (2016) 200–206.

[6] L. Chi, Q. Xu, X. Liang, J. Wang, X. Su, Iron-based metal-organic frameworks as catalysts for visible light-driven water oxidation, Small 12 (2016) 1351–1358.

[7] Q. Xu, H. Li, F. Yue, L. Chi, J. Wang, Nanoscale cobalt metal-organic framework as a catalyst for visible light-driven and electrocatalytic water oxidation, New J. Chem. 40 (2016) 3032–3035.

[8] F. Jiao, H. Frei, Nanostructured cobalt and manganese oxide clusters as efficient water oxidation catalysts, Energy Environ. Sci. 3 (2010) 1018–1027.

[9] J. Rosen, G.S. Hutchings, F. Jiao, Ordered mesoporous cobalt oxide as highly efficient oxygen evolution catalyst, J. Am. Chem. Soc. 135 (2013) 4516–4521.

[10] Y. Zhao, Y. Zhang, Y. Ding, M. Chen, Hexagonal nanoplates of $NiO/CoO/Fe_2O_3$ composite acting as an efficient photocatalytic and electrocatalytic water oxidation catalyst, Dalton Trans. 44 (2015) 15628–15635.

[11] S. Goberna-Ferrón, B. Peña, J. Soriano-López, J.J. Carbó, H. Zhao, J.M. Poblet, K.R. Dunbar, J.R. Galán-Mascarós, A fast metal–metal bonded water oxidation catalyst, J. Catal. 315 (2014) 25–32.

[12] L. Wang, Coexistence and evolution of bright pulses and dark solitons in a fiber laser, Opt. Commun. 297 (2013) 129–132.

[13] G. Chen, L. Chen, S.M. Ng, T.C. Lau, Efficient chemical and visible-light-driven water oxidation using nickel complexes and salts as precatalysts, ChemSusChem 7 (2014) 127–134.

[14] F. Evangelisti, R. Guttinger, R. More, S. Luber, G.R. Patzke, Closer to photosystem II: a Co_4O_4 cubane catalyst with flexible ligand architecture, J. Am. Chem. Soc. 135 (2013) 18734–18737.

[15] X.B. Han, Z.M. Zhang, T. Zhang, Y.G. Li, W. Lin, W. You, Z.M. Su, E.B. Wang, Polyoxometalate-based cobalt-phosphate molecular catalysts for visible light-driven water oxidation, J. Am. Chem. Soc. 136 (2014) 5359–5366.

[16] H. Chen, Z. Sun, X. Liu, A. Han, P. Du, Cobalt–salen complexes as catalyst precursors for electrocatalytic water oxidation at low overpotential, J. Phys. Chem. C 119 (2015) 8998–9004.

[17] C.Y. Cummings, F. Marken, L.M. Peter, A.A. Tahir, K.G. Wijayantha, Kinetics and mechanism of light-driven oxygen evolution at thin film alpha-Fe_2O_3 electrodes, Chem. Commun. 48 (2012) 2027–2029.

[18] X. Du, Y. Ding, R. Xiang, X. Xiang, Ferromagnetic nanocrystallines containing copper as an efficient catalyst for photoinduced water oxidation, Phys. Chem. Chem. Phys. 17 (2015) 10648–10655.

[19] D. Gonzalez-Flores, I. Sanchez, I. Zaharieva, K. Klingan, J. Heidkamp, P. Chernev, P.W. Menezes, M. Driess, H. Dau, M.L. Montero, Heterogeneous water oxidation: surface activity versus amorphization activation in cobalt phosphate catalysts, Angew. Chem. 54 (2015) 2472–2476.

[20] X.B. Han, Y.G. Li, Z.M. Zhang, H.Q. Tan, Y. Lu, E.B. Wang, Polyoxometalate-based nickel clusters as visible light-driven water oxidation catalysts, J. Am. Chem. Soc. 137 (2015) 5486–5493.

[21] G. La Ganga, F. Puntoriero, Artificial photosynthesis: a molecular approach to photo-induced water oxidation, Pure Appl. Chem. 87 (2015) 583–599.

[22] Z. Huang, Z. Luo, Y.V. Geletii, J.W. Vickers, Q. Yin, D. Wu, Y. Hou, Y. Ding, J. Song, D.G. Musaev, C.L. Hill, T. Lian, Efficient light-driven carbon-free cobalt-based molecular catalyst for water oxidation, J. Am. Chem. Soc. 133 (2011) 2068–2071.

[23] R. Schiwon, K. Klingan, H. Dau, C. Limberg, Shining light on integrity of a tetracobalt-polyoxometalate water oxidation catalyst by X-ray spectroscopy before and after catalysis, Chem. Commun. 50 (2014) 100–102.

[24] F. Song, Y. Ding, B. Ma, C. Wang, Q. Wang, X. Du, S. Fu, J. Song, $K_7[Co^{III}Co^{II}(H_2O)W_{11}O_{39}]$: a molecular mixed-valence Keggin polyoxometalate catalyst of high stability and efficiency for visible light-driven water oxidation, Energy Environ. Sci. 6 (2013) 1170.

[25] T. Zhou, D. Wang, S.C.-K. Goh, J. Hong, J. Han, J. Mao, R. Xu, Bio-inspired organic cobalt (ii) phosphonates toward water oxidation, Energy Environ. Sci. 8 (2015) 526–534.

[26] Y. Zhao, J. Lin, Y. Liu, B. Ma, Y. Ding, M. Chen, Efficient light-driven water oxidation catalyzed by a mononuclear cobalt (iii) complex, Chem. Commun. 51 (2015) 17309–17312.

[27] R. Xiang, Y. Ding, J. Zhao, Visible-light-induced water oxidation mediated by a mononuclear-cobalt(II)-substituted silicotungstate, Chem.- Asian J. 9 (2014) 3228–3237.

[28] H. Wang, Y. Lu, E. Mijangos, A. Thapper, Photo-induced water oxidation based on a mononuclear cobalt (II) complex, Chin. J. Chem. 32 (2014) 467–473.

[29] Q. Yin, J.M. Tan, C. Besson, Y.V. Geletii, D.G. Musaev, A.E. Kuznetsov, Z. Luo, K.I. Hardcastle, C.L. Hill, A fast soluble carbon-free molecular water oxidation catalyst based on abundant metals, Science 328 (2010) 342–345.

[30] S. Wang, Y. Hou, S. Lin, X. Wang, Water oxidation electrocatalysis by a zeolitic imidazolate framework, Nanoscale 6 (2014) 9930–9934.

[31] J.-W. Wang, P. Sahoo, T.-B. Lu, Re-investigation of water oxidation catalyzed by a dinuclear cobalt-polypyridine complex: identification of CoO_x as a real heterogeneous catalyst, ACS Catal. 6 (2016) 5062–5068.

[32] M. Natali, S. Berardi, A. Sartorel, M. Bonchio, S. Campagna, F. Scandola, Is $[Co_4(H_2O)_2(\alpha-PW_9O_{34})_2]^{10-}$ a genuine molecular catalyst in photochemical water oxidation? Answers from time-resolved hole scavenging experiments, Chem. Commun. 48 (2012) 8808–8810.

[33] J.J. Stracke, R.G. Finke, Electrocatalytic water oxidation beginning with the cobalt polyoxometalate $[Co_4(H_2O)_2(PW_9O_{34})_2]^{10-}$: identification of heterogeneous CoO_x as the dominant catalyst, J. Am. Chem. Soc. 133 (2011) 14872–14875.

[34] S. Fu, Y. Liu, Y. Ding, X. Du, F. Song, R. Xiang, B. Ma, A mononuclear cobalt complex with an organic ligand acting as a precatalyst for efficient visible light-driven water oxidation, Chem. Commun. 50 (2014) 2167–2169.

[35] D. Hong, J. Jung, J. Park, Y. Yamada, T. Suenobu, Y.-M. Lee, W. Nam, S. Fukuzumi, Water-soluble mononuclear cobalt complexes with organic ligands acting as precatalysts for efficient photocatalytic water oxidation, Energy Environ. Sci. 5 (2012) 7606.

[36] J.W. Vickers, H. Lv, J.M. Sumliner, G. Zhu, Z. Luo, D.G. Musaev, Y.V. Geletii, C.L. Hill, Differentiating homogeneous and heterogeneous water oxidation catalysis: confirmation that $[Co_4 (H_2O)_2(\alpha-PW_9O_{34})_2]^{10-}$ is a molecular water oxidation catalyst, J. Am. Chem. Soc. 135 (2013) 14110–14118.

[37] Y. Fan, G. Li, W. Jian, M. Yu, L. Wang, Z. Tian, S. Tianyou, S. Feng, Solvothermal synthesis crystal structure, magnetic and luminescent properties of $(H_3O)_6 \cdot [Co_4(H_2O)_4(HPMIDA)_2(PMIDA)_2)] \cdot 2H_2O$, J. Solid State Chem. 178 (2005) 2267–2273.

[38] M.W. Kanan, D.G. Nocera, In situ formation of an oxygen-evolving catalyst in neutral water containing phosphate and Co^{2+}, Science 321 (2008) 1072–1075.

[39] C. Creutz, N. Sutin, Reaction of tris (bipyridine) ruthenium (III) with hydroxide and its application in a solar energy storage system, Proc. Natl. Acad. Sci. 72 (1975) 2858–2862.

[40] P.K. Ghosh, B.S. Brunschwig, M. Chou, C. Creutz, N. Sutin, Thermal and light-induced reduction of the ruthenium complex cation $Ru(bpy)_3^{3+}$ in aqueous solution, J. Am. Chem. Soc. 106 (1984) 4772–4783.

[41] M. Hara, C.C. Waraksa, J.T. Lean, B.A. Lewis, T.E. Mallouk, Photocatalytic water oxidation in a buffered tris (2,2'-bipyridyl) ruthenium complex-colloidal IrO_2 system, J. Phys. Chem. A 104 (2000) 5275–5280.

[42] G. La Ganga, F. Puntoriero, S. Campagna, I. Bazzan, S. Berardi, M. Bonchio, A. Sartorel, M. Natali, F. Scandola, Light-driven water oxidation with a molecular tetra-cobalt (III) cubane cluster, Faraday Discuss. 155 (2012) 177–190.

[43] N.D. Morris, T.E. Mallouk, A high-throughput optical screening method for the optimization of colloidal water oxidation catalysts, J. Am. Chem. Soc. 124 (2002) 11114–11121.

[44] D. Hong, Y. Yamada, A. Nomura, S. Fukuzumi, Catalytic activity of $NiMnO_3$ for visible light-driven and electrochemical water oxidation, Phys. Chem. Chem. Phys. 15 (2013) 19125–19128.